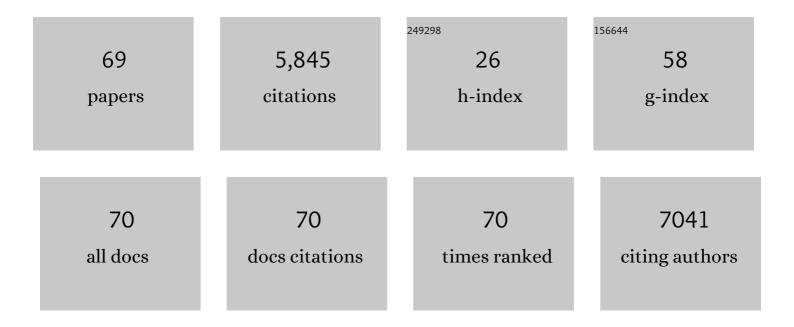
Xiang Yang Kong

List of Publications by Year in descending order

Source: https://exaly.com/author-pdf/7496409/publications.pdf Version: 2024-02-01



#	Article	IF	CITATIONS
1	Ultraâ€thin bifacial passivated emitter and rear cell with inverted pyramid textures. Physica Status Solidi (A) Applications and Materials Science, 2022, 219, 2100481.	0.8	0
2	New HPDC Mg-RE based alloy with exceptional strength and creep resistance at elevated temperature. Materials Science & Engineering A: Structural Materials: Properties, Microstructure and Processing, 2022, 840, 142921.	2.6	15
3	Tuning morphology, composition and oxygen reduction reaction (ORR) catalytic performance of manganese oxide particles fabricated by l³-radiation induced synthesis. Journal of Colloid and Interface Science, 2021, 583, 71-79.	5.0	29
4	A novel die-casting Mg alloy with superior performance: Study of microstructure and mechanical behavior. Materials Science & Engineering A: Structural Materials: Properties, Microstructure and Processing, 2021, 802, 140655.	2.6	14
5	Volume-matched ferroelectric and piezoelectric ZnO/MgO superlattice. Journal of Alloys and Compounds, 2021, 876, 160167.	2.8	7
6	Inverted Pyramid Morphology Control by Acid Modification and Application for PERC Solar Cells. ACS Omega, 2021, 6, 32925-32929.	1.6	1
7	Enhancement of ionic conductivity in novel LiON-AlOx multilayer heterostructures prepared by atomic layer deposition. Solid State Ionics, 2021, 373, 115796.	1.3	0
8	Effect of ε-Al3Ni phase on mechanical properties of Al–Si–Cu–Mg–Ni alloys at elevated temperature. Materials Science & Engineering A: Structural Materials: Properties, Microstructure and Processing, 2020, 772, 138794.	2.6	32
9	Effect of thermal exposure on microstructure and mechanical properties of Alâ^'Siâ^'Cuâ^'Niâ^'Mg alloy produced by different casting technologies. Transactions of Nonferrous Metals Society of China, 2020, 30, 1717-1730.	1.7	21
10	Mechanical properties and yield asymmetry of Mg-Y-Zn alloys: Competitive behavior of second phases. Materials Characterization, 2020, 164, 110301.	1.9	19
11	Effect of Sc microalloying addition on microstructure and mechanical properties of as-cast Al–12Si alloy. Materials Science & Engineering A: Structural Materials: Properties, Microstructure and Processing, 2019, 766, 138343.	2.6	22
12	Effect of δ-Al3CuNi phase and thermal exposure on microstructure and mechanical properties of Al-Si-Cu-Ni alloys. Journal of Alloys and Compounds, 2019, 791, 1015-1024.	2.8	45
13	Black silicon Schottky photodetector in sub-bandgap near-infrared regime. Optics Express, 2019, 27, 3161.	1.7	24
14	A proton conductor electrolyte based on molten CsH ₅ (PO ₄) ₂ for intermediate-temperature fuel cells. RSC Advances, 2018, 8, 5225-5232.	1.7	19
15	Microstructure, tensile properties and creep behavior of Al-12Si-3.5Cu-2Ni-0.8Mg alloy produced by different casting technologies. Journal of Materials Science and Technology, 2018, 34, 1222-1228.	5.6	54
16	Enzyme-catalysed room temperature and atmospheric pressure synthesis of metal carbonate hydroxides for energy storage. Nano Energy, 2018, 54, 200-208.	8.2	24
17	High areal capacitance and rate capability using filled Ni foam current collector. Electrochimica Acta, 2018, 281, 761-768.	2.6	10
18	Phases Formation and Evolution at Elevated Temperatures of Al–12Si–3.8Cu–2Ni–1Mg Alloy. Advanced Engineering Materials, 2017, 19, 1600623.	1.6	15

#	Article	IF	CITATIONS
19	Effect of Q-Al 5 Cu 2 Mg 8 Si 6 phase on mechanical properties of Al-Si-Cu-Mg alloy at elevated temperature. Materials Science & Engineering A: Structural Materials: Properties, Microstructure and Processing, 2017, 693, 26-32.	2.6	53
20	High area-specific capacitance of Co(OH) ₂ /hierarchical nickel/nickel foam supercapacitors and its increase with cycling. Journal of Materials Chemistry A, 2017, 5, 7968-7978.	5.2	80
21	A flexible phosphosilicate-based intermediate temperature composite electrolyte membrane with proton conductivity at temperatures of up to 250ŰC. International Journal of Hydrogen Energy, 2017, 42, 28829-28835.	3.8	4
22	Nanosize stabilized Li-deficient Li2â^'xO2 through cathode architecture for high performance Li-O2 batteries. Nano Energy, 2016, 27, 577-586.	8.2	42
23	A Flexible CsH5(PO4)2-Doped Composite Electrolyte Membrane for Intermediate-Temperature Fuel Cells. Journal of the Electrochemical Society, 2016, 163, F1309-F1316.	1.3	4
24	A lithium ion conductor in Li4SiO4-Li3PO4-LiBO2 ternary system. Solid State Ionics, 2016, 293, 72-76.	1.3	5
25	Nanoscale Nitrogen Doping in Silicon by Self-Assembled Monolayers. Scientific Reports, 2015, 5, 12641.	1.6	36
26	An effective way to simultaneous realization of excellent optical and electrical performance in largeâ€scale Si nano/microstructures. Progress in Photovoltaics: Research and Applications, 2015, 23, 964-972.	4.4	29
27	Atomic layer deposition for photovoltaics: applications and prospects. , 2015, , .		1
28	Type II hybrid structures of TiO2 nanorods conjugated with CdS quantum dots: assembly and optical properties. Applied Physics A: Materials Science and Processing, 2014, 114, 605-609.	1.1	3
29	Synthesis and optoelectrical properties of SnO2 nanospheres derived by microwave-assisted hydrothermal method. Applied Physics A: Materials Science and Processing, 2014, 116, 1959-1962.	1.1	2
30	Monodisperse porous LiFePO4/C microspheres derived by microwave-assisted hydrothermal process combined with carbothermal reduction for high power lithium-ion batteries. Journal of Power Sources, 2014, 258, 246-252.	4.0	79
31	Electrochemical performances of nonstoichiometric Li1+xFePO4 microspheres by microwave-assisted hydrothermal synthesis. Materials Letters, 2014, 120, 76-78.	1.3	7
32	Electrostatic assembly of CdTe quantum dots with different charged ligands into TiO2 porous film for solar cells. Applied Physics A: Materials Science and Processing, 2014, 114, 1153-1160.	1.1	6
33	One-pot Microwave Hydrothermal Synthesis of Monodisperse Core–Shell-Structured SnO2@C Microspheres. Chemistry Letters, 2014, 43, 231-233.	0.7	0
34	Microwave-assisted synthesis of water-dispersed CdTe/CdSe core/shell type II quantum dots. Nanoscale Research Letters, 2011, 6, 399.	3.1	23
35	High proton-conducting monolithic phosphosilicate glass membranes. Microporous and Mesoporous Materials, 2011, 138, 63-67.	2.2	27
36	Energy model and band-gap modulation of graphene band self-organized on the functional vicinal surfaces. Applied Physics Letters, 2011, 98, 013104.	1.5	1

XIANG YANG KONG

#	Article	IF	CITATIONS
37	Photoluminescence and Characterization of ZnO/Zn ₂ SnO ₄ Nanocables. Wuji Cailiao Xuebao/Journal of Inorganic Materials, 2011, 26, 597-601.	0.6	2
38	Facile conversion of silicon nitride nanobelts into sandwich-like nanosaws II: growth mechanism and optical properties. Applied Physics A: Materials Science and Processing, 2010, 98, 321-326.	1.1	0
39	Electrochemical performance of LiFePO4 nanorods obtained from hydrothermal process. Materials Characterization, 2010, 61, 720-725.	1.9	39
40	Energy Model and Nonlinear Bandgap Modulation of Graphene Sheet Self-Organized on the Vicinal Surfaces. International Journal of Nonlinear Sciences and Numerical Simulation, 2010, 11, .	0.4	0
41	The fabrication and characteristics of indium-oxide covered porous InP. Nanotechnology, 2009, 20, 425302.	1.3	4
42	Facile conversion of silicon nitride nanobelts into sandwich-like nanosaws: towards functional nanostructured materials. Applied Physics A: Materials Science and Processing, 2009, 97, 729-734.	1.1	8
43	Flutelike Porous Hematite Nanorods and Branched Nanostructures: Synthesis, Characterisation and Application for Gasâ€Sensing. Chemistry - A European Journal, 2008, 14, 5996-6002.	1.7	144
44	Phase Evolution in Heat-Treated Si3N4with Additions of Yb2O3. Journal of the American Ceramic Society, 2008, 91, 611-614.	1.9	3
45	Facile Synthesis and Characterization of Gallium Oxide (β-Ga ₂ O ₃) 1D Nanostructures: Nanowires, Nanoribbons, and Nanosheets. Crystal Growth and Design, 2008, 8, 1940-1944.	1.4	43
46	Atomistic Failure Mechanism of Single Wall Carbon Nanotubes with Small Diameters. Chinese Physics Letters, 2007, 24, 165-168.	1.3	7
47	Epitaxial growth of manganese silicide nanowires on Si(111)-7×7 surfaces. Applied Physics Letters, 2007, 90, 133111.	1.5	25
48	Visible light response of tin oxide nanobelts. , 2007, , .		0
49	Assembly of Metallic Carbon Nanodots Aligned on a Vicinal Si(111)-7×7 Surface. Journal of the American Chemical Society, 2007, 129, 3782-3783.	6.6	3
50	Direct measurement of residual stresses and their effects on the microstructure and mechanical properties of heat-treated Si3N4 ceramics II: With CeO2 as a single additive. Acta Materialia, 2007, 55, 3245-3251.	3.8	12
51	Integration of metal oxide nanobelts with microsystems for nerve agent detection. Applied Physics Letters, 2005, 86, 063101.	1.5	127
52	Doping and planar defects in the formation of single-crystal ZnO nanorings. Physical Review B, 2004, 70, .	1.1	84
53	Thermal Conductivities of Individual Tin Dioxide Nanobelts. , 2004, , 457.		0
54	Semiconducting and Piezoelectric Oxide Nanostructures Induced by Polar Surfaces. Advanced Functional Materials, 2004, 14, 943-956.	7.8	537

XIANG YANG KONG

#	Article	IF	CITATIONS
55	Metalâ^'Semiconductor Znâ^'ZnO Coreâ^'Shell Nanobelts and Nanotubes. Journal of Physical Chemistry B, 2004, 108, 570-574.	1.2	219
56	Interface and defect structures of Zn–ZnO core–shell heteronanobelts. Journal of Applied Physics, 2004, 95, 306-310.	1.1	72
57	Thermal conductivities of individual tin dioxide nanobelts. Applied Physics Letters, 2004, 84, 2638-2640.	1.5	123
58	Polar-surface dominated ZnO nanobelts and the electrostatic energy induced nanohelixes, nanosprings, and nanospirals. Applied Physics Letters, 2004, 84, 975-977.	1.5	284
59	Single-Crystal Nanorings Formed by Epitaxial Self-Coiling of Polar Nanobelts. Science, 2004, 303, 1348-1351.	6.0	1,383
60	Integration of metal-oxide nanobelts with microsystems for sensor applications. , 2004, , .		1
61	Polar Surfaces Induced Asymmetric Growth of Wurtzite Nanobelts. Microscopy and Microanalysis, 2004, 10, 362-363.	0.2	0
62	Directed Assembly of Metal Oxide Nanobelts With Microsystems Into Integrated Nanosensors. , 2004, , .		0
63	In Situ Structure Evolution from Cu(OH)2Nanobelts to Copper Nanowires. Journal of Physical Chemistry B, 2003, 107, 8275-8280.	1.2	84
64	Rectangular Single-Crystal Mullite Microtubes. Advanced Materials, 2003, 15, 1445-1449.	11.1	35
65	Structures of indium oxide nanobelts. Solid State Communications, 2003, 128, 1-4.	0.9	67
66	Spontaneous Polarization-Induced Nanohelixes, Nanosprings, and Nanorings of Piezoelectric Nanobelts. Nano Letters, 2003, 3, 1625-1631.	4.5	1,077
67	Induced Growth of Asymmetric Nanocantilever Arrays on Polar Surfaces. Physical Review Letters, 2003, 91, 185502.	2.9	697
68	Microwave sintering behaviour of ZrO2-Y2O3 with agglomerate. Journal of Materials Science Letters, 1996, 15, 1158-1160.	0.5	10
69	Spontaneous polarization induced growth of ZnO nanostructures. , 0, , .		1